



Effects of propofol pretreatment on lung morphology and heme oxygenase-1 expression in oleic acid-induced acute lung injury in rats¹

Zelong Tan^I, Huaizhou Wang^{II}, Jing Sun^{III}, Mingsheng Li^{IV}

^IMaster, Department of Anesthesiology, Tai'an Central Hospital, Tai'an, Shandong, China. Conception, design, intellectual and scientific content of the study; manuscript writing; critical revision.

^{II}Bachelor, Department of Anesthesiology, Yantai Stomatological Hospital, Yantai, Shandong, China. Scientific content of the study, acquisition of data.

^{III}Bachelor, Obstetrics and Gynecology, Tai'an Maternal and Child Health Hospital, Tai'an, Shandong, China. Acquisition of data.

^{IV}Master, Department of Anesthesiology, Tai'an Central Hospital, Tai'an, Shandong, China. Intellectual and scientific content of the study, critical revision.

Abstract

Purpose: To investigate the effects of propofol pretreatment on lung morphology and heme oxygenase-1 expression in oleic acid-induced acute lung injury in rats.

Methods: A total of 32 male Sprague-Dawley rats (250–300g) were randomly divided into the following four groups (n=8/group): group C, group OA, group OA+PR, and group OA+IX to compare related parameter changes.

Results: PaO₂, PCO₂, and PaO₂/FiO₂ were significantly different among the four treatment groups (P<0.05 or P<0.01). Lung wet/dry weight ratio and HO-1 protein expression also significantly differed among the groups (P<0.01). Immunohistochemistry showed that the expression of HO-1 in group OA+PR was stronger than those in groups OA, OA+IX, and C. Light microscopy revealed that pathological changes in lung tissues in group OA+PR were milder than those in group OA and group OA+IX. Electron microscopy showed that alveolar type II epithelial cell ultrastructure in group OA was relatively irregular with cell degeneration and disintegration and cytoplasmic lamellar bodies were vacuolized. Changes in group OA+PR were milder than those in group OA; however, they were more severe in group OA+IX than in group OA.

Conclusion: Propofol significantly increases the expression of HO-1 in the lung tissue and prevents changes in lung morphology due to ALI in rats.

Key words: Propofol. Heme Oxygenase-1. Acute Lung Injury. Morphology. Rats.

■ Introduction

Acute lung injury (ALI) is a critical condition characterized by severe hypoxemia and respiratory distress. Conventional treatment measures do not effectively improve prognosis in such patients¹. ALI is associated with innate immunity in ischemia-reperfusion injury², traumatic brain injury³, and septic shock⁴. Systemic inflammation is the fundamental cause of ALI⁵. Because the prevention of oxidative stress is reported to be beneficial in ALI, the expression of heme oxygenase-1 (HO-1) is also presumed to be associated with ALI⁶.

Propofol is a fat-soluble intravenous anesthetic that exerts good antioxidant effects; its lung-protective roles have also been verified⁷⁻⁹. It can regulate innate immunity and the expression of proinflammatory signals in sepsis^{10,11}. It can also reduce the expression of toll-like receptor 2/4 in sepsis^{12,13}, attenuate the expression of NF- κ B in sepsis¹⁴, and upregulate the expression of HO-1¹⁵. Although propofol is known to increase the expression of HO-1 in ALI, its effects on morphological changes in the lungs remain unexplored. This study investigated the impact of propofol on the histomorphology of the lung in oleic acid (OA)-induced ALI in rats and explored its possible mechanisms of action, aiming to provide evidence for clinical treatment.

Propofol is a fat-soluble intravenous anesthetic that exerts good antioxidant effects; its lung-protective roles have also been verified⁷⁻⁹. It can regulate innate immunity and the expression of proinflammatory signals in sepsis^{10,11}. It can also reduce the expression of toll-like receptor 2/4 in sepsis^{12,13}, attenuate the expression of NF- κ B in sepsis¹⁴, and upregulate the expression of HO-1¹⁵. Although propofol is known to increase the expression of HO-1 in ALI, its effects on morphological changes in the lungs remain unexplored. This study investigated the impact of propofol on the

histomorphology of the lung in oleic acid (OA)-induced ALI in rats and explored its possible mechanisms of action, aiming to provide evidence for clinical treatment.

■ Methods

The study was approved by the ethics committee of Tai'an Central Hospital, Tai'an, Shandong, China.

This study was carried out in strict accordance with the recommendations in the Guide for the Care and Use of Laboratory Animals of the National Institutes of Health¹⁶. The animal use protocol has been reviewed and approved by the Institutional Animal Care and Use Committee (IACUC) of Tai'an Central Hospital. All procedures were performed in accordance with the Declaration of Helsinki of the World Medical Association¹⁷.

Sample collection

Arterial blood (0.5ml) was withdrawn from the internal carotid artery, and dissolved gases in the blood were analyzed by a GEMpremierTM3000 blood gas analyzer (US Instrumentation Laboratory Company). After blood withdrawal, all rats were euthanized by cervical dislocation. Further, the left lung of each rat was isolated. The wet (W) and dry (D) weights (followed by 72h drying to a constant weight at 80°C) were noted, and the W/D weight ratio was calculated. The median lobe of the right lung of each rat was cut into a 0.3×0.3×0.5cm portion and fixed in 10% neutral formalin (pH 7.2–7.4) for 24h for immunohistochemical and HE staining. Histopathological findings were reported and double-checked by three different blinded pathologists.

Immunohistochemistry results

Immunohistochemistry was performed

using a ready-to-use two-step (non-biotin) test kit. Rabbit anti-rat primary antibodies, goat anti-rabbit secondary antibodies, and DAB chromogenic agent were purchased from Beijing ZSGB-Bio Origene Co., Ltd. A Leica DM1000 microscope (LeicaDFCT6.5.0 Switzerland Ltd.) was used to obtain images, which were analyzed for the integral optical density of HO-1 protein using the image-Pro Plus 6.0 optical analysis system. Each tissue section was sampled at five different fields and the average value was calculated.

Nine right lung lobes (1x1x1mm) were also randomly sampled, followed by fixation in 2.5% glutaraldehyde. After rinsing twice with 0.1M PBS (10min/rinse), they were post-fixed with 1% osmic acid for 2h, treated with acetone gradient dehydration, and embedded by epoxy Resin 618. Ultrathin sections were prepared and stained stepwise with uranium dye and lead; the ultrastructure of the alveolar type II epithelial cells (AEC-II) was then observed using a Philips TECNAI10 electron microscope (the Netherlands Philips company).

Statistical analysis

All data analyses were performed using

the SPSS13.0 statistical software; data are expressed as the mean±standard deviation. Inter groups differences were analyzed using one-way ANOVA followed by the LSD (when the variance was homogeneous) or Dunnett T3 (when the variance was non-homogeneous) *post hoc* test, with P<0.05 considered as statistically significant.

Results

PaO₂, PCO₂, and PaO₂/FiO₂

PaO₂ and PaO₂/FiO₂ in all ALI groups were significantly lower than those in group C (P<0.01); however, PCO₂ was significantly higher (P<0.01). PaO₂ and PaO₂/FiO₂ in group OA+PR were significantly different from those in group C (P>0.05). PaO₂ and PaO₂/FiO₂ in group OA+PR were significantly higher than those in group OA (P<0.01); however, PCO₂ was significantly lower (P<0.01). PaO₂ and PaO₂/FiO₂ in group OA+IX were significantly lower than those in group OA (P<0.01 or P<0.05) (Table 1).

Table 1 - Arterial blood gas analysis after injecting OA for 120min ($\bar{x} \pm s$, n=8).

Group	PaO ₂	PCO ₂	PaO ₂ /FiO ₂
C	92.15±1.23	39.65±1.77	438.65±5.89
OA	56.15±4.36 ^{▲▲}	60.62±4.01 ^{▲▲}	266.08±20.56 ^{▲▲}
OA+ PR	91.20±1.21 ^{★★}	46.25±1.99 ^{▲▲★★}	431.02±5.50 ^{★★}
OA+IX	50.48±1.69 ^{▲▲★}	58.23±2.23 ^{▲▲}	239.78±8.01 ^{▲▲★}

Compared with group C, ^{▲▲}P<0.01; compared with group OA, ^{★★}P<0.01, [★]P<0.05.

Lung W/D weight ratio, lung injury score, and HO-1 protein expression

Lung W/D weight ratio, lung injury score, and HO-1 protein expression in all ALI groups were significantly higher than those in group C (P<0.05 or P<0.01). Lung W/D weight ratio and lung injury score in group OA+PR

were significantly lower than those in group OA (P<0.05 or P<0.01); however, HO-1 protein expression was significantly higher (P<0.01). Group OA+IX exhibited significantly increased lung W/D weight ratio and lung injury score (P<0.05) but significantly decreased HO-1 protein expression (P<0.01) (Table 2).

Table 2 - Comparison of W/ D, lung injury score and IOD of HO-1 protein expression among different groups ($\bar{x} \pm s$, n=8).

Group	W/D	lung injury score	HO-1
C	3.66±0.05	0.86±0.43	3.55±0.14
OA	5.79±0.20 ^{▲▲}	2.65±0.55 [▲]	4.77±0.04 ^{▲▲}
OA+ PR	4.76±0.15 ^{▲▲▲*}	1.53±0.51 ^{▲*}	5.15±0.06 ^{▲▲▲*}
OA+IX	5.96±0.16 ^{▲▲*}	2.84±0.53 ^{▲*}	4.28±0.12 ^{▲▲*}

Compared with group C, ^{▲▲} $P < 0.01$, [▲] $P < 0.05$; compared with group OA, ^{▲▲} $P < 0.01$, ^{*} $P < 0.05$.

Light microscopy of the lung tissue

The gross specimen images are shown in Figure 1. A clear lung structure was seen in group C; the alveolar septal capillaries were mildly expanded and congested, and the partial alveolar septa and bronchial stroma exhibited a small degree of lymphocyte infiltration. The lung tissue in group OA was damaged; the alveolar septal capillaries were markedly expanded and congested, scattered small focal bleeding was observed, and coagulated lung necrotic foci of different sizes were present.

The structure of the lung tissue in group OA+PR was still clear; the alveolar septal capillaries were expanded and congested with only mild edema in the alveolar cavity. The structure of the lung tissue in group OA+IX was damaged; the alveolar septal capillaries were markedly expanded and congested, the alveolar cavity was partially filled with edema fluid, extensive lymphocyte infiltration (with few neutrophils) was observed in the partial alveolar septum, and coagulated lung necrotic foci of different sizes were observed (Figure 1).

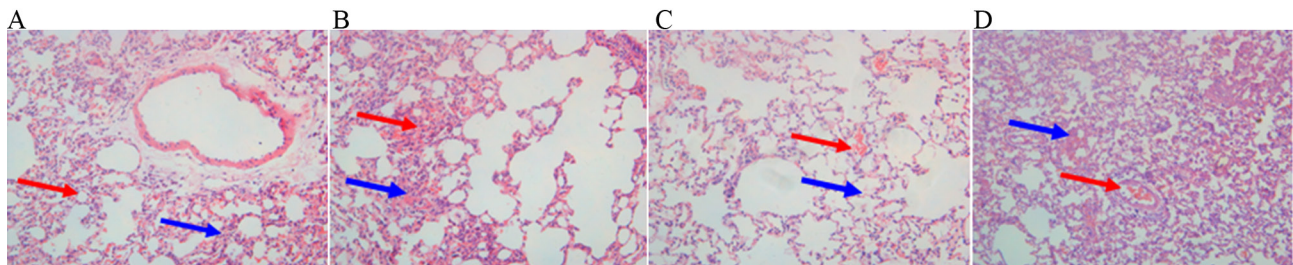


Figure 1 - **A**: Clear lung structure can be seen, the alveolar septal capillaries mildly expand and congest, and partial alveolar septum and bronchial stroma exhibit a small amount of lymphocyte infiltration; **B**: The structure of lung tissue is unclear, the alveolar septal capillaries expand and congest, together with scattered small focal bleeding and coagulated lung necrotic foci with different sizes; **C**: The structure of lung tissue is still clear, the alveolar septal capillaries expand and congest, and a small amount of edema fluid can be seen in the alveolar cavity; **D**: The structure of lung tissue is unclear, the alveolar septal capillaries exhibit high-degree expansion and congestion, partial alveolar cavity is filled with edema fluid, partial alveolar septum have the infiltration of a large number of lymphocytes and a small amount of neutrophils, together with coagulated lung necrotic foci with different sizes (HE staining x200).

HO-1 protein expression in the lung tissue

HO-1 protein in group OA+PR was strongly expressed in the bronchial cells, AECs,

and alveolar macrophages; however, it was weakly expressed in groups OA, OA+IX, and C (Figure 2).

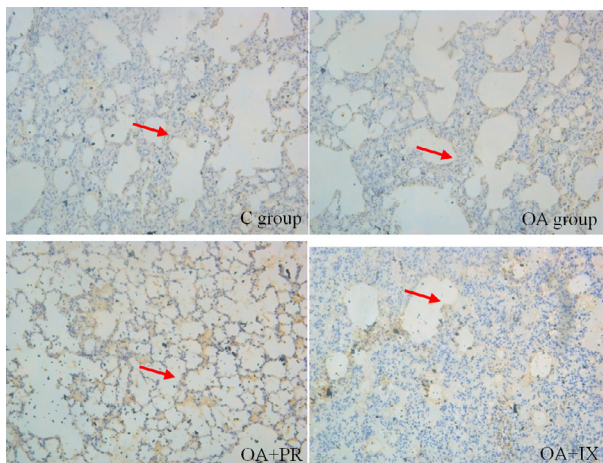


Figure 2 - The expression of HO-1 protein: OA+PR group was strong positive; OA group and OA+IX group, the expression was positive with OA+IX group was weaker; the expression in C group was weakly positive.

AEC-II ultrastructure

Electron microscopy revealed regular

AEC-II shape in group C; the cell surface was covered with microvilli of different lengths and thicknesses, the nuclei were conspicuous, and the cytoplasm contained various lamellar bodies in different numbers, sizes, and maturation stages. Group OA exhibited relatively irregular AEC-II shape, cell degeneration, and disintegration; the microvilli on the cell surface were reduced in number, and the cytoplasmic lamellar bodies were emptied (partially into the alveolar cavity). Group OA+PR exhibited relatively regular AEC-II shape, the microvilli were reduced in number, the nuclei were conspicuous, and the cytoplasm contained various lamellar bodies in different numbers and sizes. Group OA+IX exhibited irregular AEC-II, cell degeneration, and disintegration; no microvilli were seen on the cell surface, and the cytoplasmic lamellar bodies were emptied and vacuolized (Figure 3).

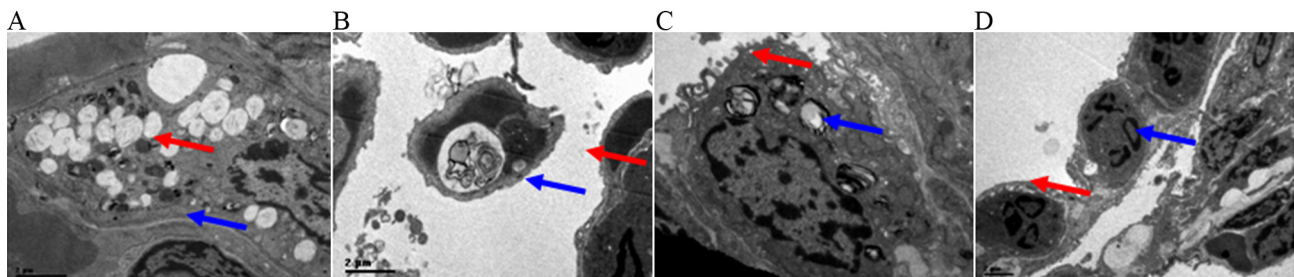


Figure 3 - **A:** Regular AEC-II shape in group C, the cell surface is covered with microvilli with different lengths and thickness, the nuclei are obvious, and the cytoplasm contains various lamellar bodies with different numbers and sizes, different maturation stages of which can also be seen; **B:** Group OA exhibits relatively irregular AEC-II shape, cell degeneration, or even disintegration; the microvilli on the cell surface are reduced, the cytoplasmic lamellar bodies are emptied (partially into alveolar cavity); **C:** Group OA+ PR exhibits relatively regular AEC-II shape, the microvilli are reduced, the nuclei are obvious, the cytoplasm contains various lamellar bodies with different numbers and sizes; **D:** Group OA+IX exhibits irregular AEC-II, cell degeneration, or even disintegration, no microvilli can be seen on the cell surface, and the cytoplasmic lamellar bodies are emptied and vacuolized. Ultrastructure of AEC-II (red arrow: microvilli, blue arrow: lamellar bodies).

Discussion

Results of this study show that OA injection induced ALI in rats in a dose- and

time-dependent manner^{18,19}. OA-induced ALI presents an early phase of necrosis and microvascular thrombosis, followed by a repair phase with the proliferation of type II cells

and fibrotic foci in subpleural areas²⁰. The analysis of arterial blood gas PaO₂ in group OA showed a progressive decline in respiratory capacity and significant cyanosis with the PaO₂/FiO₂<300mmHg. The lung W/D weight ratio increased, and pathological damage was evident in the lung tissue, which also indicated alveolar space telangiectasia with scattered small focal bleeding without coagulation necrosis, alveolar collapse, and atrophy. These changes indicate ALI.

In this study, we evaluated the impact of propofol on OA-induced ALI in rats. Consistent with results of previous studies²¹, results of this study show that propofol can significantly reduce OA-induced ALI. We also found that HO-1 was strongly expressed in the propofol-pretreated lung tissue, which can significantly improve PaO₂, significantly decrease lung W/D weight ratio, lung injury, and apoptosis of AT-II in OA rats. Zinc porphyrin IX also exhibited this effect, suggesting that HO-1 is involved in the anti-apoptotic action of propofol. Propofol pretreatment significantly reduced edema of the lung tissue^{21,22}.

Previous studies have shown that propofol can inhibit inflammatory response by inhibiting reactive oxygen species-regulated Akt/IKKβ/NF-κB signaling²³ and reduce endotoxin-induced ALI^{24,25}. Because the etiology of ALI is complex, the protective effect of propofol on OA-induced ALI needs to be further investigated. HO-1 plays a key role in ALI^{26,27}. HO-1-based treatment strategies in ALI may be more meaningful, and drug discovery in this direction will increase our treatment options. Therefore, we aimed to identify the process by which propofol upregulates HO-1 expression to relieve OA-induced lung morphological changes in ALI.

ALI is a dynamic pathophysiological process that injures the lung tissue. Although

currently used treatment measures to control or eliminate causes of ALI, including pulmonary protective ventilation, the rational application of antibiotics, liquid intake control, and continuous blood purification, exist, the prognosis of ALI/acute respiratory distress syndrome (ALI/ARDS) remains a challenge²⁴. Therefore, there is a need to further investigate the occurrence and development mechanisms of ALI/ARDS and possible effective interventions. Based on previous studies²¹, we presumed that propofol has a protective effect on OA-induced ALI. This is the first study performed to compare the effects of propofol and zinc porphyrin IX pretreatment on ALI in terms of HO-1 expression and lung histomorphology. We found that PaO₂ and PaO₂/FiO₂ in group OA+PR were significantly higher than those in group OA (P<0.01); however, lung W/D weight ratio and lung injury score were significantly lower (P<0.01 and P<0.05, respectively). The expression of HO-1 protein was significantly higher in group OA+PR than in group OA (P<0.01), indicating that propofol induces the expression of HO-1. Zinc porphyrin IX (specific inhibitor of HO) was found to reduce HIF-1α expression and inhibit hypoxia-mediated VEGF release and cell proliferation²⁸ in group OA+IX. PaO₂ and PaO₂/FiO₂ were significantly lower in group OA+IX than in group OA (P<0.05), whereas the lung W/D weight ratio and lung injury score were significantly higher than in group OA (P<0.01 and P<0.05, respectively). The expression of HO-1 was significantly lower in group OA+IX than in group OA (P<0.01), which showed that HO-1 expression was inhibited by zinc porphyrin IX. Consequently, the high expression of HO-1 in group OA+PR was related to propofol, which is consistent with related reports²⁵⁻²⁹. This effect was confirmed by lung histomorphology analysis by light microscopy and AEC- II ultrastructure

analysis by electron microscopy. The results of this study have high clinical importance in the diagnosis and treatment of ALI patients; however, because the results are mainly based on animal experiments, further human trials are necessary.

■ Conclusion

The pretreatment with propofol promotes the expression of HO-1 in the lung tissue and significantly prevents changes in lung morphology due to ALI.

■ References

1. Neamu RF, Martin GS. Fluid management in acute respiratory distress syndrome. *Curr Opin Crit Care*. 2013 Feb;19(1):24-30. doi: 10.1097/MCC.0b013e32835c285b.
2. Jing H, Yao J, Liu X, Fan H, Zhang F, Li Z, Tian X, Zhou Y. Fish-oil emulsion (omega-3 polyunsaturated fatty acids) attenuates acute lung injury induced by intestinal ischemia-reperfusion through Adenosine 5'-monophosphate-activated protein kinase-sirtuin1 pathway. *J Surg Res*. 2014 Mar;187(1):252-61. doi: 10.1016/j.jss.2013.10.009.
3. Song Z, Zhao X, Gao Y, Liu M, Hou M, Jin H, Cui Y. Recombinant human brain natriuretic peptide ameliorates trauma-induced acute lung injury via inhibiting JAK/STAT signaling pathway in rats. *J Trauma Acute Care Surg*. 2015 May;78(5):980-7. doi: 10.1097/TA.0000000000000602.
4. Lin WC, Chen CW, Huang YW, Chao L, Chao J, Lin YS, Lin CF. Kallistatin protects against sepsis-related acute lung injury via inhibiting inflammation and apoptosis. *Sci Rep*. 2015 Jul 22;5:12463. doi: 10.1038/srep12463.
5. Dzierba AL, Abel EE, Buckley MS, Lat I. A review of inhaled nitric oxide and aerosolized epoprostenol in acute lung injury or acute respiratory distress syndrome. *Pharmacotherapy*. 2014 Mar;34(3):279-90. PMID: 24734313.
6. Shiva S, Oh JY, Landar AL, Ulasova E, Venkatraman A, Bailey SM, Darley-Usmar VM. Nitroxia: the pathological consequence of dysfunction in the nitric oxid-cytochrome oxidase signaling pathway. *Free Radic Biol Med*. 2005 Feb 1;38(3):297-306. doi: 10.1016/j.freeradbiomed.2004.10.037.
7. Zhang L, Jin J, Yao J, Yue Z, Wei Y, Yang W, Fu S, Li W. Effects of propofol on excitatory and inhibitory amino acid neurotransmitter balance in rats with neurogenic pulmonary edema induced by subarachnoid hemorrhage. *Neurocrit Care*. 2016 Jun;24(3):459-71. doi: 10.1007/s12028-015-0206-x.
8. Zhao W, Zhou S, Yao W, Gan X, Su G, Yuan D, Hei Z. Propofol prevents lung injury after intestinal ischemia-reperfusion by inhibiting the interaction between mast cell activation and oxidative stress. *Life Sci*. 2014 Jul 17;108(2):80-7. doi: 10.1016/j.lfs.2014.05.009.
9. Yang P, Yang N, Zhang X, Xu X. The significance and mechanism of propofol on treatment of ischemia reperfusion induced lung injury in rats. *Cell Biochem Biophys*. 2014 Dec;70(3):1527-32. doi: 10.1007/s12013-014-0088-0.
10. Bao HG, Li S. Effects of propofol on the outcomes of rats with sepsis. *J Surg Res*. 2011 Jun 1;168(1):e111-5. doi: 10.1016/j.jss.2010.12.034.
11. Tang J, Hu JJ, Lu CH, Liang JN, Xiao JF, Liu YT, Lin CS, Qin ZS. Propofol inhibits lipopolysaccharide-induced tumor necrosis factor-alpha expression and myocardial depression through decreasing the generation of superoxide anion in cardiomyocytes. *Oxid Med Cell Longev*. 2014;2014:157376. doi: 10.1155/2014/157376.
12. Schläpfer M, Piegeler T, Dull RO, Schwartz DE, Mao M, Bonini MG, Z'Graggen BR, Beck-Schimmer B, Minshall RD. Propofol increases morbidity and mortality in a rat model of sepsis. *Crit Care*. 2015 Feb 19;19:45. doi: 10.1186/s13054-015-0751-x.
13. Ma L, Wu XY, Zhang LH, Chen WM, Uchiyama A, Mashimo T, Fujino Y. Propofol exerts anti-inflammatory effects in rats with lipopolysaccharide-induced acute

- lung injury by inhibition of CD14 and TLR4 expression. *Braz J Med Biol Res.* 2013 Mar;46(3):299-305. PMID: 23532269.
14. Wang T, Wei XY, Liu B, Wang LJ, Jiang LH. Effects of propofol on lipopolysaccharide-induced expression and release of HMGB1 in macrophages. *Braz J Med Biol Res.* 2015 Apr;48(4):286-91. doi: 10.1590/1414-431X20144222.
15. Liang C, Cang J, Wang H, Xue Z. Propofol attenuates cerebral ischemia/reperfusion injury partially using heme oxygenase-1. *J Neurosurg Anesthesiol.* 2013 Jul;25(3):311-6. doi: 10.1097/ANA.0b013e31828c6af5.
16. National Research Council (US) Committee for the Update of the Guide for the Care and Use of Laboratory Animals. *Guide for the care and use of laboratory animals.* Washington (DC): National Academies Press; 2011.
17. World Medical Association. *World Medical Association Declaration of Helsinki. Ethical principles for medical research involving human subjects.* *Bull World Health Organ.* 2001;79(4):373-4. PMID: 15835069.
18. Ulrich K, Stern M, Goddard ME, Williams J, Zhu J, Dewar A, Painter HA, Jeffery PK, Gill DR, Hyde SC, Geddes DM, Takata M, Alton EW. Keratinocyte growth factor therapy in murine oleic acid-induced acute lung injury. *Am J Physiol Lung Cell Mol Physiol.* 2005 Jun;288(6):L1179-92. doi: 10.1152/ajplung.00450.2004.
19. Zhao LL, Hu GC, Zhu SS, Li JF, Liu GJ. Propofol pretreatment attenuates lipopolysaccharide-induced acute lung injury in rats by activating the phosphoinositide-3-kinase/Akt pathway. *Braz J Med Biol Res.* 2014 Dec;47(12):1062-7. PMID: 25387673.
20. Lai JP, Bao S, Davis IC, Knoell DL. Inhibition of the phosphatase PTEN protects mice against oleic acid-induced acute lung injury. *Br J Pharmacol.* 2009 Jan;156(1):189-200. doi: 10.1111/j.1476-5381.2008.00020.x.
21. Gonçalves-de-Albuquerque CF, Silva AR, Burth P, Castro-Faria MV, Castro-Faria-Neto HC. Acute respiratory distress syndrome: role of oleic acid-triggered lung injury and inflammation. *Mediators Inflamm.* 2015;2015:260465. doi: 10.1155/2015/260465.
22. Zhao LL, Hu GC, Zhu SS, Li JF, Liu GJ. Propofol pretreatment attenuates lipopolysaccharide-induced acute lung injury in rats by activating the phosphoinositide-3-kinase/Akt pathway. *Braz J Med Biol Res.* 2014 Dec;47(12):1062-7. doi: 10.1590/1414-431X20143949.
23. Yao W, Luo G, Zhu G, Chi X, Zhang A, Xia Z, Hei Z. Propofol activation of the Nrf2 pathway is associated with amelioration of acute lung injury in a rat liver transplantation model. *Oxid Med Cell Longev.* 2014;2014:258567. doi: 10.1155/2014/258567.
24. Hsing CH, Lin MC, Choi PC, Huang WC, Kai JI, Tsai CC, Cheng YL, Hsieh CY, Wang CY, Chang YP, Chen YH, Chen CL, Lin CF. Anesthetic propofol reduces endotoxic inflammation by inhibiting reactive oxygen species-regulated Akt/IKK β /NF- κ B signaling. *PLoS One.* 2011 Mar 8;6(3):e17598. doi: 10.1371/journal.pone.0017598.
25. Gokcinar D, Ergin V, Cumaoglu A, Menevse A, Aricioglu A. Effects of ketamine, propofol, and ketofol on proinflammatory cytokines and markers of oxidative stress in a rat model of endotoxemia-induced acute lung injury. *Acta Biochim Pol.* 2013;60(3):451-6. PMID: 24020061.
26. Chen HG, Xie KL, Han HZ, Wang WN, Liu DQ, Wang GL, Yu YH. Heme oxygenase-1 mediates the anti-inflammatory effect of molecular hydrogen in LPS-stimulated RAW 264.7 macrophages. *Int J Surg.* 2013;11(10):1060-6. doi: 10.1016/j.ijssu.2013.10.007.
27. Wang J, Yang H, Hu X, Fu W, Xie J, Zhou X, Xu W, Jiang H. Dobutamine-mediated heme oxygenase-1 induction via PI3K and p38 MAPK inhibits high mobility group box 1 protein release and attenuates rat myocardial ischemia/reperfusion injury in vivo. *J Surg Res.* 2013 Aug;183(2):509-16. doi: 10.1016/j.jss.2013.02.051.
28. Ma L, Wu XY, Zhang LH, Chen WM, Uchiyama A, Mashimo T, Fujino Y. Propofol exerts anti-inflammatory effects in rats with lipopolysaccharide-induced acute lung injury by inhibition of CD14 and TLR4 expression. *Braz J Med Biol Res.* 2013 Mar;46(3):299-305. doi: 10.1590/1414-431X20122379.

29.Cheng CC, Guan SS, Yang HJ, Chang CC, Luo TY, Chang J, Ho AS. Blocking heme oxygenase-1 by zinc protoporphyrin reduces tumor hypoxia-mediated VEGF release and inhibits tumor angiogenesis as a potential therapeutic agent against colorectal cancer. *J Biomed Sci.* 2016 Jan 28;23:18. doi: 10.1186/s12929-016-0219-6.

Correspondence:

Mingsheng Li
Department of Anesthesiology, Tai'an Central
Hospital
Tai'an 271000 Shandong China
Phone: +86 538 6298552
cnmingshengli@126.com

Conflict of interest: none

Financial source: none

Received: Nov 27, 2017

Review: Jan 26, 2018

Accepted: Feb 28, 2018

¹Research performed at Center Laboratory,
Tai'an Central Hospital, Shandong, China.

